Biogeosciences
Discussions

Open Access

EGU

Fungal loop transfer of N depends on biocrust constituents and N form

2

Zachary T. Aanderud[1], Trevor B. Smart[1], Nan Wu[2], Alexander S. Taylor[1],

4   **Yuanming Zhang[2], Jayne Belnap[3]**

6   [1]Department of Plant and Wildlife Sciences, Brigham Young University, Provo, Utah

84602, USA

8   [2]Xinjiang Institute of Ecology and Geography, Key Laboratory of Biogeography and

Bioresource in Arid Land, Chinese Academy of Sciences, Urumqi 830011, China

10   [3]US Geological Survey, Southwest Biological Science Center, 2290 S. Resource

Blvd., Moab, UT 84532, USA

12

Running head: dark septate fungi translocate ammonium in biocrusts

14

Correspondence to: Zachary T. Aanderud (zachary_aanderud@byu.edu)

18

20   **Abstract.**   Besides performing multiple ecosystem services individually and

collectively, biocrust constituents may also create biological networks connecting

22   spatially and temporally distinct processes. In the fungal loop hypothesis, rainfall

variability allows fungi to act as conduits and reservoirs, translocating resources

24   between soils and host plants. To evaluate the extent biocrust species composition and

N form influence loops, we created a minor, localized rainfall event containing

26   $^{15}NH_4^+$ and $^{15}NO_3^-$ and measured the resulting $\delta^{15}N$ in surrounding cyanobacteria- and

lichen-dominated crusts and grass, *Achnatherum hymenoides*, after twenty-four hours.

28   We also estimated the biomass of fungal constituents using quantitative PCR and

characterized fungal communities by sequencing the 18S rRNA gene. We only found

30   evidence of fungal loops in cyanobacteria-dominated crusts where ^{15}N, from $^{15}NH_4^+$,

moved 40 mm h^{-1} and the $\delta^{15}N$ in crusts decreased as the radial distance from the

32   water addition increased (linear regression analysis: $R^2=0.58$, $F=16$, $P=0.002$, $n=14$).

In cyanobacteria crusts, $\delta^{15}N$, from $^{15}NH_4^+$, was diluted as Ascomycota biomass

34   increased (linear regression analysis: $R^2=0.50$, $F=8.8$, $P=0.02$, $n=14$), Ascomycota

accounted for 82% (±2.8) of all fungal sequences, and one order, Pleosporales,

36   comprised 66% (±6.9) of Ascomycota. The lack of loops in moss-dominated crusts

and substantial movement of $^{15}NO_3^-$ may stem from mosses effectively sequestering

38   newly fixed N and fungi preferring $^{15}NH_4^+$ for amino acid transformation and

translocation. No label entered *A. hymenoides*. Our findings suggest that minor

40   rainfall events allow dark septate Pleosporales to rapidly translocate N in the absence

of a plant sink.

1   Introduction

42

Fungi may act as conduits for biological networks connecting belowground

44   ecosystem processes to plants. Soil fungi contribute to all aspects of litter

decomposition through the generation of a myriad of extracellular enzymes (Osono

46   2007, Schneider et al. 2012); altered trophic dynamics, decomposer species diversity,

and nutrient turnover rates (Hattenschwiler et al. 2005); and by forming multiple

48   types of endophyte-plant symbioses (Johnson et al. 1997, Saikkonen et al. 2004).

Endophytic fungi ,in particular, form hubs connecting spatially and temporally

50   distinct microbial-mediated soil processes and plants. For example, the pervasive

distribution of mycorrhizae in mesic systems allows common mycorrhizal networks

52   to deliver essential resources, which promotes or hinders seedling growth depending

on the network species composition (van der Heijden and Horton 2009), and

54   facilitates the one-way transfer of multiple forms of N and P between two plant

species linked by arbuscular mycorrhizae and ectomycorrhizae (He et al. 2003,

56   Walder et al. 2012). In xeric systems, endophytic fungi are also implicated in moving

resources within biological networks in a theory known as the fungal loop hypothesis.

58   The hypothesis states that fungi, supported by biotrophic C from plants and

cyanobacteria, act as intermediate reservoirs transforming and translocating resources

60   between soils and plants (Collins et al. 2008, 2014)). Perhaps the most notable

example of a fungal loop, albeit from a limited number of studies, occurred in

62   fungal-dominated cyanobacteria biocrusts from a Chihuahuan Desert grassland.

Specifically, $^{15}NO_3^-$ applied to a root-free biocrust rapidly moved into the perennial

64   grass, *Bouteloua* species, up to 1 m away within 24–hours (Green et al. 2008).

       Furthermore, ^{13}C-labeled glutamic acid applied to leaf surfaces of *Bouteloua* was

66   found in biocrusts. Despite the intriguing evidence, many aspects of this burgeoning

       hypothesis remain to be validated (Collins et al. 2014).

68

       Biocrust composition and soil moisture availability interactions may dictate the

70   movement of resources in fungal loops. Desert fungal-plant interactions occur across

       spatially discontinuous patches of vegetation interspersed by patches of soils

72   colonized by biocrusts (Belnap et al. 2005). Fungi participating in loops are

       necessarily associated with a mosaic of other biocrust organisms (i.e., cyanobacteria,

74   green algae, lichens, mosses, and other bacteria). The metabolic activity of biocrust

       constituents participating in fungal loops, including plants, are moisture-dependent

76   and regulated by the magnitude and seasonality of episodic rainfall events. A

       pulse-reserve paradigm (Collins et al. 2008) may explain biological activities where

78   minor rainfall pulses stimulate microorganisms, generating reserves of resources to be

       exploited during subsequent rainfall events (Huxman et al. 2004, Welter et al. 2005).

80   In such loops, minor rainfall events may stimulate N_2 fixation by free or

       lichen-associated cyanobacteria (Belnap et al. 2003), N mineralization by bacteria and

82   fungi (Cable and Huxman 2004, Yahdjian and Sala 2010) and nitrification and possibly

       denitrification (Wang et al. 2014) all increasing the levels of NH_4^+ or NO_3^-. Fungal

84   species, including fungal endophytes, may compete with mosses, lichen,

       cyanobacteria, and other bacteria for newly released N. Once sequestered, the N may be

86 transformed into amino acids and transported within mycelium (Jin et al. 2012, Behie

and Bidochka 2014). Larger rainfall events may then activate plants, allowing the host

88 to receive N from the fungi and transfer photosynthate to the fungal endophyte. If

fungal endophytes are poor competitors for newly released N, preferentially sequester

90 one inorganic N form over another, or more efficiently transform and transport NH_4^+ or

NO_3^-, biocrust constituents and N form may influence the translocation of N in fungal

92 loops.

94 The fungal endophytes most likely involved in the loop hypothesis are dark septate

fungi. Few arbuscular mycorrhizal fungi are found in biocrusts (Porras-Alfaro et al.

96 2011) or as endophytes in desert plants (Titus et al. 2002), due to mycorrhizae being

relatively sensitive to dry soil conditions (Aguilera et al. 2016). In contrast, the

98 majority of biocrust fungi are Ascomycota, with the Pleosporales being widespread

and dominant (Bates et al. 2012, Porras-Alfaro et al. 2011). Pleosporales, along with

100 other Ascomycota fungal orders, contain dark septate endophytes (Jumpponen and

Trappe 1998). Dark septate are thermal- and drought-tolerant fungi due to

102 melanin-rich cell walls conferring protection from UV and drought stress (Gostincar

et al. 2010). Taken together, the prevalence of dark septate fungi in desert systems,

104 along with their ability to maintain metabolic activity under low water potentials

(Barrow 2003), makes these endophytes excellent candidates to translocate resources

106 in loops (Green et al. 2008).

108   Minor rainfall events may allow fungi to act as conduits and reservoirs for N. To

investigate the potential for biocrust constituents and N form to influence the

110   movement of N through the putative fungal loops, we created minor, localized rainfall

events and measured $\delta^{15}N$, from $^{15}N-NH_4^+$ and $^{15}N-NO_3^-$, within surrounding

112   cyanobacteria- and moss-dominated crusts, and grass, *Achnatherum hymenoides*

(Indian ricegrass). In tandem with ^{15}N analyses, we estimated the biomass of two

114   major division of fungi (Ascomycota and Basidiomycota) and bacteria, and

characterized fungal communities by sequencing the 18S rRNA gene to identify

116   potential link between fungal taxa and ^{15}N movement.

118   **2   Materials and methods**

2.1 Site description

120   We conducted our study in two cold desert ecosystems of the Colorado Plateau, UT.

One site was near Castle Valley (40°05'27.43"N-112°18'18.24"W) and the other was

122   adjacent to the US Geological Survey (USGS), Southwest Biological Science Center

Research Station in Moab, UT (40°05'27.43"N-112°18'18.24"W). Rugose crusts

124   consisting of moss *Syntrichia caninervis* and cyano-lichens *Collema tenax* and

Collema coccophorum cover the Castle Valley site (Darrouzet-Nardi et al. 2015),

126   while smooth, light algal crusts of one cyanobacterium, *Microcoleus vaginatus*, cover

the USGS site. Specifically, biocrust cover across the Castle Valley was 50%

128   cyanobacteria, 22% *S. caninervis*, and 5-7% *Collema* spp. (Zelikova et al. 2012), and

100% cyanobacteria for the USGS. Across both sites, vegetation is dominated by

Biogeosciences
Discussions

130 perennial grass *Achnatherum hymenoides* (Roem & Schult) and native perennial

shrub *Atriplex confertifolia* (Torr. & Frém). Mean annual temperature and

132 precipitation at Castle Valley is 13ºC and 269 mm, while the USGS site is slightly

warmer (MAT=13.8ºC) and drier (MAP=189 mm; based on 1981-2010 data; WRCC

134 2017). Both soils are Aridisols with Castle Valley classified as a sandy loam,

calcareous Rizno series (Darrouzet-Nardi et al. 2015) and USGS as a Bluechief series

136 sandy loam.

138 **2.2 Simulated rainfall events and ^{15}N form applications**

We simulated rainfall events containing two isotopically-labeled, inorganic N forms

140 and tracked the movement of the label through our moss-dominated (Castle Valley)

and cyanobacteria-dominated biocrusts (USGS Station), and *A. hymenoides*. First, we

142 randomly selected six circular plots per site with a radius of 1.0 m and at least 10 m

apart from each other. Three plots were assigned to be labeled with K^{15}NO$_3$ (99 at.%)

144 and the other three plots to be labeled with (^{15}NH$_4$)$_2$SO$_4$ (99 at.%). Second, we

randomly selected five biocrust and five *A. hymenoides* along eight axes (e.g., N, NE,

146 E, SE, S, SW, W, and NW) radiating from the center of each circular plot and

measured the radial distance to biocrusts or grasses. Third, we simulated a 2.5 mm

148 rainfall event by spraying 3 mL of deionized water solution and either isotopic label

(0.30 mg ^{15}N) onto a 5 cm diameter circle in the center of the circular plots (2 biocrust

150 types × 3 circular plots locations × 2 N forms × ≈10 samples [5 biocrusts or 4–8 *A.

hymenoides* depending on grass density in the circular plot]=137). The ^{15}N additions

152   wetted the sandy loams (bulk density≈1.5 g cm^{-3}) to a depth of 1 cm and added

approximately equal NH_4^+ and double NO_3^- concentrations to surface soils (Sperry et

154   al. 2006). All additions were completed midday in April as *A. hymenoides* were

starting to set seed.

156

2.3 Sample collection and ^{15}N analyses

158   Biocrust and foliage samples were collected twenty-four hours after the simulated

rainfall event containing our different inorganic ^{15}N forms. Biocrusts were removed

160   as three subsamples from each biocrust location with a soil corer (2 cm diameter × 5

cm length) to a depth of 2 mm. Crust distances away from the tracer application

162   ranged from 22–97 cm. The composited soil sample was kept cold (5°C) in the field,

split in the lab, and a portion of the soil was frozen (-20°C) until we performed fungal

164   and bacterial DNA analyses. We randomly selected five leaves from *Achnatherum*,

which ranged in distance anywhere from 29–120 cm away from the tracer application

166   and in volume from 0.002–0.048 m^3. The leaves and remaining soils (sieved 2 mm)

were air-dried, ground in a reciprocating tissue homogenizer, and analyzed for ^{15}N

168   using a PDZ Europa ANCA-GSL elemental analyzer, interfaced with a PDZ Europa

20–20 isotope ration mass spectrometer (Sercon Ltd., Cheshire, UK) at the University

170   of California Davis Stable Isotope Facility (http://stableisotopefacility.ucdavis.edu).

We expressed the resulting isotope ratios in δ notation as parts per thousand (‰)

172   where:

$$\delta^{15}N = (R_{sample} / R_{standard}) \times 1000 \qquad\qquad (1)$$

174   R is the molar ratio of the heavier to the lighter isotope (^{15}N/^{14}N) for the standard or

sample. To track the movement of inorganic N forms through our two biocrust types

176   (moss-lichen-dominated and cyanobacteria dominated biocrust) and into grasses, we

analyzed the relationships between δ^{15}N present in crust and leaf tissue to the distance

178   of the crust and *Achnatherum* by site using linear regression in SigmaPlot Version

13.0 (Systat Software, San Jose, CA).

180

2.4 Biomass estimations of major fungal components

182   To investigate the potential for fungi to translocate our ^{15}N forms, we estimated the

biomass of two major divisions of fungi (Ascomycota and Basidiomycota) and

184   bacteria in biocrusts using quantitative PCR. From the frozen biocrust samples, we

extracted genomic DNA using a DNeasy PowerLyzer PowerSoil Kit (Qiagen, MD,

186   USA) and quantified the gene copy numbers of Ascomycota and Basidiomycota on a

Mastercycler EP Realplex qPCR (Eppendorf, Hamburg, Germany) with SYBR Green.

188   We amplified division-specific regions of the internal transcribed spacer (ITS) with

primer pair ITS5 (forward) and ITS4A (reverse) for Ascomycota (Larena et al. 1999)

190   and ITS4B (forward) and 5.8sr (reverse) for Basidiomycota (Fierer et al. 2005). We

selected the universal bacterial 16S rRNA primer set EUB 338, forward, and Eub518,

192   reverse, to estimate the biomass of bacteria (Aanderud et al. 2013). In 12.5 μl

reactions, using KAPA2G Robust PCR Kits (KAPA Biosystems, Wilmington, MA,

194   USA), we amplified targeted genes using the following thermocycler condition: an

initial denaturation step at 94ºC for 3 min followed by 35 cycles of denaturation at

196   94ºC for 45 s, annealing at either at 55 ºC (Ascomycota), 64ºC (Basidiomycota), or

60ºC (bacteria) for 30 s, and extension at 72ºC for 90 sec. We generated qPCR

198   standards for Basidiomycota, Ascomycota, and bacteria from biocrusts using the

TOPO TA Cloning® Kit (ThermoFisher Scientific, MA, USA) as outlined by

200   Aanderud et al. (2013). The coefficients of determination (R^2) for our assays ranged

from 0.90 to0.99, and amplification efficiencies fell between 0.99 and 1.92. We

202   analyzed the relationships between biocrust $\delta^{15}N$ and the gene copy number of

Ascomycota and Basidiomycota using linear regression to investigate the potential for

204   fungi to act as conduits for inorganic N. We tested for differences in our biomass

estimates between the crust types using multiple t-tests and a Benjamini-Hochberg

206   correction to control for the false discovery rate associated with multiple comparisons

(Benjamini and Hochberg 1995).

208

2.5 Biocrust fungal communities

210   To identify the fungal taxa participating in N translocation, we characterized fungal

communities in biocrusts using bar-coded sequencing. We PCR amplified the V9

212   region of the 18S rRNA gene using a universal eukaryote primer set, 1391F and

EukBr, with a unique 12-bp Golay barcode fused to EukBr (Amaral-Zettler et al. 2009,

214   Hamady et al. 2008). Thermocycler parameters were similar to qPCR analyses and

consisted of a denaturation step at 94°C for 3 min, followed by 35 cycles of

216   denaturation at 94°C for 45 s, an annealing step at 57°C for 60 s, elongation at 72°C for

90 s, and a final extension at 72°C for 10 min. We then purified and pooled PCR

218   amplicon libraries to near equimolar concentrations using SequalPrep™ Normalization

Plate Kits (Invitrogen, Carlsbad, CA, USA) and quantified the amplicon libraries by

220   real-time qPCR using a KAPA Library Quantification Kit (Kapa Biosystems,

Wilmington, MA, USA). All samples were sequenced at the Brigham Young

222   University DNA Sequencing Center (http://dnasc.byu.edu/) using the Illumina HiSeq

2500 platform (Illumina Biotechnology, San Diego, CA, USA), generating 2×250

224   paired-end reads. Illumina sequence reads were analyzed within QIIME (v. 1.9.1), an

open-source software pipeline suitable for microbial community analysis (Caporaso et

226   al. 2010). We removed barcodes and primers with a custom, in-house script previous to

joining paired-end reads by using fastq-join under default parameters (Aronesty 2011).

228   Joined reads were then de-multiplexed and checked for chimeras (Haas et al. 2011). We

then clustered the de-multiplexed reads into OTUs, applying a similarity threshold of

230   97%, using QIIME's default OTU clustering tool-uclust (Edgar et al. 2011).

Taxonomies of representative OTUs were assigned using uclust and the 18S rRNA

232   gene SILVA 128 database which was clustered into OTUs at 97% similarity (Quast et

al. 2013). To evaluate if biocrust type supported similar fungal composition, we

234   calculated the relative recovery of 27 fungal orders, including dark septate lineages. We

tested for differences between biocrust types using t-tests and a Benjamini-Hochberg

236   correction.

238   **3   Results**

3.1 Translocation of $^{15}NH_4^+$ in cyanobacteria biocrusts

240   The movement of ^{15}N was most dramatic in cyanobacteria-dominated biocrusts

following the addition of ^{15}NH$_4^+$. In cyanobacteria crusts, δ^{15}N decreased as the radial

242   distance from the central application point of ^{15}NH$_4^+$ increased (R^2=0.58, F=16,

P=0.002, n=14, figure 1A). Surrounding the tracer application, δ^{15}N was enriched

244   upwards of 40‰ more than 20 cm away and continued to be enriched to

approximately 10‰ almost 100 cm away. To a lesser extent, ^{15}NO$_3^-$ followed a

246   similar pattern. δ^{15}N decreased as the radial distance from the central application

point of ^{15}NO$_3^-$ in cyanobacteria crusts increased, but the δ^{15}N was never more

248   enriched than 8‰ (R^2=0.17, F=2.6, P<0.0001, n=15, figure 1B).

     In moss-dominated biocrusts, there was no relationship between δ^{15}N and the

250   radial distance from either the ^{15}NH$_4^+$ (R^2=0.01, F=0.13, P=0.73, n=15, figure 1A) or

^{15}NO$_3^-$ addition (R^2=0.03, F=0.46, P=0.51, n=15, figure 1B). There was no

252   relationship between δ^{15}N found in *A. hymenoides* leaves and the radial distance from

the ^{15}NH$_4^+$ or ^{15}NO$_3^-$ application with δ^{15}N in leaves ranging from 3–18‰. The R^2

254   and F values from the regressions between leaves δ^{15}N and isotopic distance was

0.01–0.21 and 0.14–2.6 (n=14–23) respectively (data not shown).

256

3.2 ^{15}NH$_4^+$ movement in cyanobacteria biocrusts related to Ascomycota

258   The biocrust that translocated N also exhibited a robust relationship between

Ascomycota biomass and biocrust δ^{15}N. In cyanobacteria biocrusts, the greater the

260   gene copy number of Ascomycota the lower the δ^{15}N from ^{15}NH$_4^+$ (R^2=0.50, F=8.8,

P=0.02, n=14, figure 2A). Ascomycota biomass was marginally related to δ^{15}N from

Biogeosciences

Discussions

Open Access

EGU

262   $^{15}NO_3^-$ in cyanobacteria crusts (R^2=0.07, F=1.1, P=0.08, n=15, figure 2B). In moss

crusts, however, there was no such relationship between $\delta^{15}N$ from $^{15}NH_4^+$ (R^2=0.05,

264   F=1.6, P=0.24, n=15, figure 2A) and $^{15}NO_3^-$ (R^2=0.01, F=0.10, P=0.75, n=15, figure

2B) and Ascomycota biomass. Basidiomycota and bacteria biomass in both crust

266   types was not related to either N form with R^2, F, and P values ranging from 0.01–

0.10, 0.1–1.5, and 0.24–0.90 (n=12–15) respectively (data not shown). The biomass

268   of all measured biocrust components was consistently higher in moss- than

cyanobacteria-dominated crusts. Basidiomycota biomass was 1.5×10^9 ±5.5×10^8

270   (means ±SEM) in cyanobacteria and 5.8×10^9 ±7.2×10^8 in moss biocrusts (t-test, t=4.5,

P<0.0001, df=1, data not shown). Ascomycota biomass was 2.6×10^7 ±4.5×10^6 (means

272   ± SEM) in cyanobacteria and 1.1×10^8 ±2.4×10^7 in moss biocrusts (t-test, t=3.3,

P=0.003, df=1). Bacterial biomass was at least two orders of magnitude lower in

274   biocrusts (cyanobacteria=5.5×10^6 ±8.9×10^5 and moss crusts=2.7×10^7 ±4.8×10^6,

(t-test, t =4.5, P<0.0001, df=1).

276

3.3 Dark septate fungi as major components of biocrusts

278   Four of the nine fungal orders contained known dark septate endophyte members and

were present in both biocrust types with the Pleosporales and Pezizales being dominant

280   taxa. In biocrusts: fungi comprised much of eukaryotic community

(cyanobacteria=30% ±4.7 and moss=33% ±4.0), Ascomycota was the most common

282   fungal division (cyanobacteria=82% ±2.8 and moss=87% ±2.9), and orders with

known dark septate members accounted for at least 67% of the Ascomycota

284   (cyanobacteria=83% ±4.8 and moss=67% ±8.6, figure 3). In cyanobacteria biocrusts,

Pleosporales accounted for 66% (±6.9) of all dark septates and the recovery of this taxa

286   was two-times higher in cyanobacteria- than moss- dominated crusts (t-test, t=03.0,

P=0.01, df=1). Even though the relative abundance of Pleosporales differed, the

288   number of gene copies of Pleosporales were similar between the two biocrusts

(cyanobacteria=1.7×10^7 ±6.3×10^6 and moss=2.9×10^7 ±1.3×10^7, t-test, t=0.99, P=0.35,

290   df=1) as determined by an extrapolation of qPCR values in conjunction with percent

recovery of taxa for Ascomycota. The *Pezizales* comprised a relatively larger

292   percentage of the biocrust community in moss-dominated biocrust with a recovery of

15% (± 8.3) and 28% (± 9.0) in cyanobacteria- and moss-dominated crusts respectively

294   (t-test, t=1.1, P=0.32, df=1). Eukaryotic community data was based on the recovery of

1,232,312 quality sequences and 5,176 unique OTUs.

296

4   Discussion

298   In biological networks, the magnitude and direction of resource transfer in fungi is

predominantly thought to be influenced by the physiological source-sink gradients

300   created by individual plants (Fellbaum et al. 2014) or between plants (Weremijewicz

et al. 2016). However, fungi may be more than just passive conduits and exert control

302   over resources due to their own sink-source resource needs (Simard and Durall 2004).

Our finding suggest that a minor rainfall event stimulated fungi, likely dark septate

304   endophytes, to rapidly translocate N at a rate of 40 mm h^{-1} in the absence of a plant

sink for N. In the absence of a large rainfall event to stimulate plant activity, none of

306 the isotope entered *A. hymenoides*. The movement of N was only apparent in the

cyanobacteria-dominated crusts where $\delta^{15}N$ decreased as the distance from the

308 simulated rainfall event and $^{15}NH_4^+$ application increased. Further, the presence of

Ascomycota was related to biocrust $\delta^{15}N$ from $^{15}NH_4^+$ with the isotope being diluted

310 as Ascomycota biomass increased. Eighty-three percent of the Ascomycota were from

four fungal orders containing known dark septate endophytes and 66% of these taxa

312 were from one order, the Pleosporales. Taken together, our results suggest that fungal

loops are structured by fungal constituents, especially Pleosporales, translocating N

314 from NH_4^+ over NO_3^-.

316 **4.1 Fungal loops only in cyanobacteria-dominated crusts**

Although the moss, *S. caninervis*, appeared to hinder N transfer between biocrusts and

318 plants, our findings suggest that fungal loops do occur in cyanobacteria-dominated

biocrusts. Lichen-dominated biocrusts remain to be tested. Our results are consistent

320 with Green et al. (2008) whose previous work identified loops in cyanobacteria

biocrusts across the Chihuahuan Desert grassland and showed comparable distances

322 of N movement within biocrusts (Green et al. 2008=44 mm h^{-1}). Biocrust components

are known to fix and secrete up to 50% of their newly fixed C and 88% newly fixed N

324 to surrounding soils within minutes to days of fixation, depending on precipitation

characteristics (Belnap et al. 2003), and thus, would likely be available to other

326 biocrust constituents, such as fungi, for translocation. Bacteria and fungi were found

in both crust types, albeit in different amounts and species compositions, but mosses

328   mosses and lichens only occurred in one crust type. Mosses, in particular, change the

N cycling characteristics of arid lands. When *S. caninervis* was lost from this system,

330   a dramatic increase in NH_4^+, which ultimately nitrifies to NO_3^-, was observed (Reed et

al. 2012). The decomposition of dead mosses most likely contributed to the increase

332   of N; however, after the mosses died, inorganic N pooled in the remaining

cyanobacteria-dominated biocrust. Thus, mosses may be effective scavengers for N

334   and outcompete fungal endophytes for newly fixed N. The ability of mosses to

scavenge N is well recognized in other systems (Liu et al. 2013, Fritz et al. 2014).

336   Further, rhizoids, stem cells, and thalli of bryophytes may contain fungal associations

(Pressel et al. 2010). If desert mosses have fungal associations, then fungi have the

338   potential to move sequestered N to the mosses in a new kind of loop. Unlike plants

that may require a larger rainfall event to become active, fungi and mosses, including

340   *S. caninervis*, are stimulated by minor rainfall events (Wu et al. 2014) and dark

septate endophytes do colonize mosses (Day and Currah 2011). Thus, the exchange of

342   photosynthate and N may occur in a tighter, more localized loop. Another explanation

may lie in the microtopography of the two biocrusts. The moss-dominated crust was

344   pinnacled, while the cyanobacteria-dominated crust was smooth. Therefore, transport

distance between our application point and target plant was significantly further in

346   mosses than cyanobacteria crusts, potentially slowing the movement of N.

348   **4.2 Loops may preferentially move NH_4^+ over NO_3^-**

16

We found that NH_4^+, but not NO_3^-, was rapidly translocated within crusts. The

350 enrichment of $\delta^{15}N$, from $^{15}NH_4^+$, in cyanobacteria biocrusts was related to the

Ascomycota and potentially dark septate fungi due to their dominance. We explain

352 the negative relationship between Ascomycota gene copy number and $\delta^{15}N$ signal as a

simple dilution—the higher the biomass of Ascomycota, the more spread in the ^{15}N

354 signal. Although the physiology of dark septate fungi remains relatively unexplored,

if our desert fungi are like other fungi then the preferential movement of NH_4^+ is

356 understandable. Generally, fungi prefer NH_4^+ over NO_3^- (Eltrop and Marschner 1996),

as NH_4^+ is readily acquired by fungi and assimilated into amino acids. After NH_4^+

358 uptake and assimilation via the glutamate synthase or GS/GOGAT cycle, N is

incorporated into arginine through the urea cycle (Jin et al. 2012) due to the direct

360 assimilation of NH_4^+ into the GS/GOGAT pathway (Courtly et al., 2015). Thus, NH_4^+

is most likely transformed into arginine and moved within mycelium by amino acid

362 transporters (Govindarajulu et al. 2005, Garcia et al. 2016). Quantum dots

(fluorescent nanoscale semiconductors) have tracked the flow of organically derived

364 N into arbuscular mycorrhizae and into *Poa annua* in less than 24 hours (Whiteside et

al. 2009) and arbuscular colonization can also increase uptake of multiple other amino

366 acids (e.g., phenylalanine, lysine, asparagine, arginine, histidine, methionine,

tryptophan, and cysteine) by their host plants (Whiteside et al. 2012). NO_3^- did move

368 in our cyanobacteria crusts but not nearly to the extent reported by Green et al.

(2008). Besides fungal preferences, other factors may play a role in the uptake of N,

370 such as the increase in mobility of NO_3^- in soils, differences in soil cation exchange

capacity due to clay content, or fungi capitalizing on the more abundant N form

372   specific to a soil. More information is needed to identify the importance of N form

and the movement of organic N within fungal loops.

374

4.3 Dark septate and Pleosporales as conduits

376   Our results support the idea that Pleosporale*s* are the most likely conduits for N. Four

of the nine fungal orders we identified contained known dark septate endophyte

378   members but one order was the most abundant. The Pleosporales accounted for 66% of

the Ascomycota taxa in cyanobacteria crusts. Based on the relationship between $\delta^{15}N$

380   and Ascomycota biomass, the overwhelming abundance of Pleosporales, and the

universal occurrence of Ascomycota in biocrusts, the Pleosporales assumedly play a

382   role in fungal loops. We are not the first to reach this conclusion. Green et al. (2008)

also identified Pleosporale*s* as being the primary candidate involved in fungal loops. In

384   their semi-arid grassland, Pleosporale*s* were the most common taxa on *Bouteloua* roots,

in the rhizosphere, and in biocrusts. We found 799 operational taxonomic units, based

386   on 97% similarity, with all of the identifiable sequences, belonging to three genera:

Leptosphaeria (1.6% of Pleosporales sequences), *Morosphaeria* (3.8% of Pleosporales

388   sequences), and *Ophiosphaerella* (8.1% of Pleosporales sequences; data not shown).

Leptosphaeria and *Ophiosphaerella* may be pathogenic endophytes on grass species

390   (Martin et al. 2001, Yuan et al. 2017), but may also be beneficial by delaying and

reducing the symptoms of other fungal pathogens (Yuan et al. 2017). However, 86% of

392   our Pleosporales taxa were unidentifiable and potentially novel, suggesting that much

remains unknown about dark septates in deserts.

394

5. Conclusion

396   Biocrusts, potentially, are interconnected in extensive biological networks. Dark

septate endophytes may act as conduits within the network by acting as both a sink

398   and source for translocating resources. In light of the absence of N movement in

moss-dominated crusts, mosses potentially hindered fungal loops. No isotopic label

400   entered *A. hymenoides* consistent with the fungal loop hypothesis that predicts plant

activity only after a larger rainfall event. Our results add to the indirect evidence of

402   fungal loops, but more information is needed to quantify the direct translocation of N

through dark septate fungi, characterize the magnitude and directionality of resources

404   within the endophytic relationship, and demonstrate the importance of a second larger

rainfall in structuring resource exchange.

406

412

Author contributions ZTA and JB designed the study. ZTA, TBS, NW, AST, and JB

414   conducted the experiments. ZTA, TBS, NW, AST, YZ, and JB analyzed and

interpreted the data. ZTA, TBS, NW, AST, YZ, and JB helped write and review the

416   manuscript. ZTA agrees to be accountable for all aspects of the work in ensuring that

questions related to the accuracy or integrity of any part of the work are appropriately

418   investigated and resolved.

420   **Conflict of interest** The authors declare no conflict of interest.

422

Biogeosciences
Discussions

Open Access

EGU

424 **Figure legend**

Figure 1   Cyanobacteria biocrusts facilitated the translocation of N in

426 **twenty-four hours.** Based on linear regression analyses, $\delta^{15}N$, from $^{15}NH_4^+$,

(R^2=0.58, F=16, P=0.002, n=14) and to a lesser extent $^{15}NO_3^-$ (R^2=0.17, F=2.6,

428 P<0.0001, n=15), decreased as the radial distance from the isotopic application

increased. Values are $\delta^{15}N$ (‰) from two biocrust types, cyanobacteria- and

430 moss-dominated crusts, across circular plots (radius of 1.0 m) with a central

application (5 cm diameter circle) of $^{15}NH_4^+$ and $^{15}NO_3^-$.

432

Figure 2   Ascomycota biomass influenced the distance N traveled. In

434 cyanobacteria crusts, $\delta^{15}N$, from $^{15}NH_4^+$, was diluted as Ascomycota gene copy

number increased (R^2=0.50, F=8.8, P=0.02, n=14). Values are $\delta^{15}N$ (‰) from

436 biocrusts and Ascomycota gene copy numbers, an approximation of biomass, from

qPCR of the ITS region with primer pair ITS5 and ITS4A.

438

Figure 3   Pleosporales were the dominant Ascomycota order and contained

440 **dark septate species.** Pie chart values are means (n=6) of the relative recovery from

nine fungal orders, four of which contain dark septate endophytic taxa. Recovery was

442 based on OTUs from eukaryotic community libraries of the 18S rRNA gene (97%

similarity cutoff).

444

References cited

446   Aanderud ZT, Jones SE, Schoolmaster DR, Fierer N, Lennon JT. 2013. Sensitivity of

        soil respiration and microbial communities to altered snowfall. Soil Biology &

448   Biochemistry 57:217-227.

        Aguilera LE, Armas C, Cea AP, Gutierrez JR, Meserve PL, Kelt DA. 2016. Rainfall,

450   microhabitat, and small mammals influence the abundance and distribution of soil

        microorganisms in a Chilean semi-arid shrubland. Journal of Arid Environments

452   126:37-46.

        Amaral-Zettler LA, McCliment EA, Ducklow HW, Huse SM. 2009. A method for

454   studying protistan diversity using massively parallel sequencing of V9

        hypervariable regions of small-subunit ribosomal RNA genes. PLOS ONE (art.

456   e6372)

        Aronesty E. 2011. Command-line tools for processing biological sequence data.

458   *Expression Analysis*. (14 October 2017;

        https://github.com/ExpressionAnalysis/ea-utils)

460   Barrow JR. 2003. Atypical morphology of dark septate fungal root endophytes of

        Bouteloua in arid southwestern USA rangelands. Mycorrhiza 13:239-247.

462   Bates ST, Nash TH, Garcia-Pichel F. 2012. Patterns of diversity for fungal

        assemblages of biological soil crusts from the southwestern United States.

464   Mycologia 104:353-361.

        Behie SW, Bidochka MJ. 2014. Nutrient transfer in plant-fungal symbioses. Trends in

466   Plant Science 19:734-740.

Belnap J, Hawkes CV, Firestone MK. 2003. Boundaries in miniature: Two examples

468   from soil. BioScience 53:739-749.

Belnap J, Phillips SL, Sherrod SK, Moldenke A. 2005. Soil biota can change after

470   exotic plant invasion: does this affect ecosystem processes? Ecology

86:3007-3017.

472   Benjamini Y, Hochberg Y. 1995. Controlling the false discovery rate: a practical and

powerful approach to multiple testing. Journal of the Royal Statistical Society

474   Series B: (Methodological) 57:289-300.

Cable JM, Huxman TE. 2004. Precipitation pulse size effects on Sonoran Desert soil

476   microbial crusts. Oecologia 141:317-324.

Caporaso JG, et al. 2010. QIIME allows analysis of high-throughput community

478   sequencing data. Nature Methods 7:335-336.

Collins SL, Sinsabaugh RL, Crenshaw C, Green L, Porras-Alfaro A, Stursova M,

480   Zeglin LH. 2008. Pulse dynamics and microbial processes in aridland ecosystems.

Journal of Ecology 96:413-420.

482   Collins SL, et al. 2014. A multiscale, hierarchical model of pulse dynamics in

arid-land ecosystems. Annual Review of Ecology, Evolution, and Systematics

484   45:397-419.

Darrouzet-Nardi A, Reed SC, Grote EE, Belnap J. 2015. Observations of net soil

486   exchange of CO_2 in a dryland show experimental warming increases carbon losses

in biocrust soils. Biogeochemistry 126:363-378.

488   Day MJ, Currah RS. 2011. Role of selected dark septate endophyte species and other

        hyphomycetes as saprobes on moss gametophytes. Botany-Botanique 89:349-359.

490   Edgar RC, Haas BJ, Clemente JC, Quince C, Knight R. 2011. UCHIME improves

        sensitivity and speed of chimera detection. Bioinformatics 27:2194-2200.

492   Eltrop L, Marschner H. 1996. Growth and mineral nutrition of non-mycorrhizal and

        mycorrhizal Norway spruce (Picea abies) seedlings grown in semi-hydroponic

494   sand culture. New Phytologist 133:469-478.

        Fellbaum CR, Mensah JA, Cloos AJ, Strahan GE, Pfeffer PE, Kiers ET, Bucking H.

496   2014. Fungal nutrient allocation in common mycorrhizal networks is regulated by

        the carbon source strength of individual host plants. New Phytologist

498   203:646-656.

        Fierer N, Jackson JA, Vilgalys R, Jackson RB. 2005. Assessment of soil microbial

500   community structure by use of taxon-specific quantitative PCR assays. Applied

        and Environmental Microbiology 71:4117-4120.

502   Fritz C, Lamers LPM, Riaz M, van den Berg LJL, Elzenga T. 2014. Sphagnum

        mosses-masters of efficient N-uptake while avoiding intoxication. PLOS ONE

504   (art. e79991).

        Garcia K, Doidy J, Zimmermann SD, Wipf D, Courty PE. 2016. Take a trip through

506   the plant and fungal transportome of mycorrhiza. Trends in Plant Science

        21:937-950.

508   Gostincar C, Grube M, de Hoog S, Zalar P, Gunde-Cimerman N. 2010.

Extremotolerance in fungi: evolution on the edge. FEMS   Microbiology Ecology

510   71:2-11.

Govindarajulu M, Pfeffer PE, Jin HR, Abubaker J, Douds DD, Allen JW, Bucking H,

512   Lammers PJ, Shachar-Hill Y. 2005. Nitrogen transfer in the arbuscular

mycorrhizal symbiosis. Nature 435:819-823.

514   Green LE, Porras-Alfaro A, Sinsabaugh RL. 2008. Translocation of nitrogen and

carbon integrates biotic crust and grass production in desert grassland. Journal of

516   Ecology 96:1076-1085.

Haas BJ, et al. 2011. Chimeric 16S rRNA sequence formation and detection in Sanger

518   and 454-pyrosequenced PCR amplicons. Genome Research 21:494-504.

Hamady M, Walker JJ, Harris JK, Gold NJ, Knight R. 2008. Error-correcting

520   barcoded primers for pyrosequencing hundreds of samples in multiplex. Nature

Methods 5:235-237.

522   Hattenschwiler S, Tiunov AV, Scheu S. 2005. Biodiversity and litter decomposition

in terrestrial ecosystems. Annual Review of Ecology 36:191-218.

524   He XH, Critchley C, Bledsoe C. 2003. Nitrogen transfer within and between plants

through common mycorrhizal networks (CMNs). Critical Reviews in Plant

526   Sciences 22:531-567.

Huxman TE, Snyder KA, Tissue D, Leffler AJ, Ogle K, Pockman WT, Sandquist DR,

528   Potts DL, Schwinning S. 2004. Precipitation pulses and carbon fluxes in semiarid

and arid ecosystems. Oecologia 141:254-268.

530   Jin HR, Liu J, Huang XW. 2012. Forms of nitrogen uptake, translocation, and transfer

      via arbuscular mycorrhizal fungi: A review. Science ChinaLife Sciences

532   55:474-482.

      Johnson NC, Graham JH, Smith FA. 1997. Functioning of mycorrhizal associations

534   along the mutualism-parasitism continuum. New Phytologist 135:575-586.

      Jumpponen A, Trappe JM. 1998. Dark septate endophytes: a review of facultative

536   biotrophic root-colonizing fungi. New Phytologist 140:295-310.

      Larena I, Salazar O, Gonzalez V, Julian MC, Rubio V. 1999. Design of a primer for

538   ribosomal DNA internal transcribed spacer with enhanced specificity for

      ascomycetes. Journal of Biotechnology 75:187-194.

540   Liu XY, Koba K, Makabe A, Li XD, Yoh M, Liu CQ. 2013. Ammonium first: natural

      mosses prefer atmospheric ammonium but vary utilization of dissolved organic

542   nitrogen depending on habitat and nitrogen deposition. New Phytologist

      199:407-419.

544   Martin DL, Bell GE, Baird JH, Taliaferro CM, Tisserat NA, Kuzmic RM, Dobson

      DD, Anderson JA. 2001. Spring dead spot resistance and quality of seeded

546   bermudagrasses under different mowing heights. Crop Science 41:451-456.

      Osono T. 2007. Ecology of ligninolytic fungi associated with leaf litter

548   decomposition. Ecological Research 22:955-974.

      Porras-Alfaro A, Herrera J, Natvig DO, Lipinski K, Sinsabaugh RL. 2011. Diversity

550   and distribution of soil fungal communities in a semiarid grassland. Mycologia

      103:10-21.

552   Pressel S, Bidartondo MI, Ligrone R, Duckett JG. 2010. Fungal symbioses in

         bryophytes: new insights in the twenty first century. Phytotaxa 9:238-253.

554   Quast C, Pruesse E, Yilmaz P, Gerken J, Schweer T, Yarza P, Peplies J, Glockner FO.

         2013. The SILVA ribosomal RNA gene database project: improved data

556   processing and web-based tools. Nucleic Acids Research 41:D590-D596.

         Reed SC, Coe KK, Sparks JP, Housman DC, Zelikova TJ, Belnap J. 2012. Changes to

558   dryland rainfall result in rapid moss mortality and altered soil fertility. Nature

         Climate Change 2:752-755.

560   Saikkonen K, Wali P, Helander M, Faeth SH. 2004. Evolution of endophyte-plant

         symbioses. Trends in Plant Science 9:275-280.

562   Schneider T, Keiblinger KM, Schmid E, Sterflinger-Gleixner K, Ellersdorfer G,

         Roschitzki B, Richter A, Eberl L, Zechmeister-Boltenstern S, Riedel K. 2012.

564   Who is who in litter decomposition? Metaproteomics reveals major microbial

         players and their biogeochemical functions. ISME Journal 6:1749-1762.

566   Simard SW, Durall DM. 2004. Mycorrhizal networks: a review of their extent,

         function, and importance. Canadian Journal of Botany 82:1140-1165.

568   Sperry LJ, Belnap J, Evans RD. 2006. Bromus tectorum invasion alters nitrogen

         dynamics in an undisturbed arid grassland ecosystem. Ecology 87:603-615.

570   Titus JH, Titus PJ, Nowak RS, Smith SD. 2002. Arbuscular mycorrhizae of Mojave

         Desert plants. Western North American Naturalist 62:327-334.

Biogeosciences
Discussions

Open Access

EGU
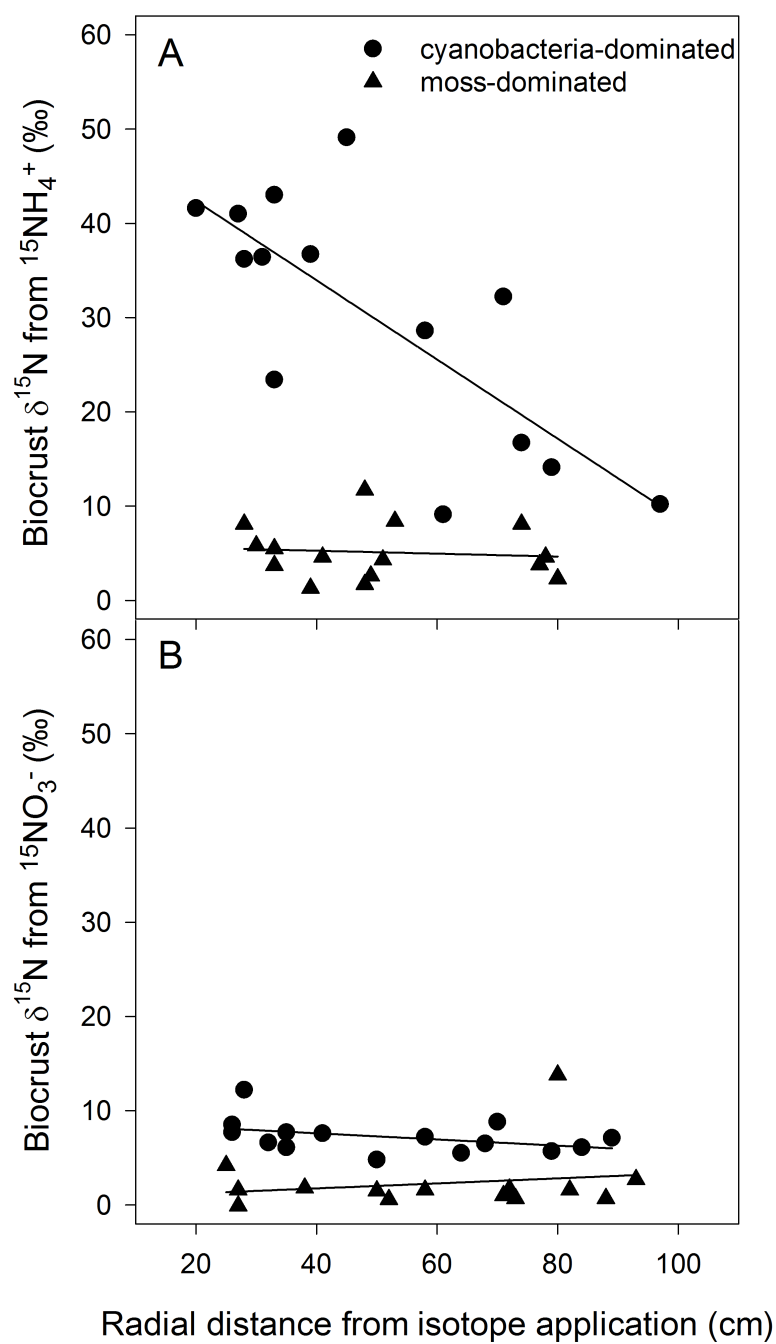
572   van der Heijden MGA, Horton TR. 2009. Socialism in soil? The importance of

mycorrhizal fungal networks for facilitation in natural ecosystems. Journal of

574   Ecology 97:1139-1150.

Walder F, Niemann H, Natarajan M, Lehmann MF, Boller T, Wiemken A. 2012.

576   Mycorrhizal networks: common goods of plants shared under unequal terms of

trade. Plant Physiology 159:789-797.

578   Wang C, et al. 2014. Aridity threshold in controlling ecosystem nitrogen cycling in

arid and semi-arid grasslands. Nature Communications (art. 4799).

580   Welter JR, Fisher SG, Grimm NB. 2005. Nitrogen transport and retention in an arid

land watershed: Influence of storm characteristics on terrestrial-aquatic linkages.

582   Biogeochemistry 76:421-440.

Weremijewicz J, Sternberg L, Janos DP. 2016. Common mycorrhizal networks

584   amplify competition by preferential mineral nutrient allocation to large host

plants. New Phytologist 212:461-471.

586   Whiteside MD, Treseder KK, Atsatt PR. 2009. The brighter side of soils: quantum

dots track organic nitrogen through fungi and plants. Ecology 90:100-108.

588   Whiteside MD, Garcia MO, Treseder KK. 2012. Amino Acid Uptake in Arbuscular

Mycorrhizal Plants. PLOS ONE (art. e47643).

590   Wu N, Zhang YM, Downing A, Aanderud ZT, Tao Y, Williams S. 2014. Rapid

adjustment of leaf angle explains how the desert moss, Syntrichia caninervis,

592   copes with multiple resource limitations during rehydration. Functional Plant

Biology 41:168-177.

594   Yahdjian L, Sala OE. 2010. Size of precipitation pulses controls nitrogen

        transformation and losses in an arid Patagonian ecosystem. Ecosystems

596   13:575-585.

        Yuan Y, Feng HJ, Wang LF, Li ZF, Shi YQ, Zhao LH, Feng ZL, Zhu HQ. 2017.

598   Potential of endophytic fungi isolated from cotton roots for biological control

        against verticillium wilt disease. PLOS ONE (art. e0170557):12.

600   Zelikova TJ, Housman DC, Grote EE, Neher DA, Belnap J. 2012. Warming and

        increased precipitation frequency on the Colorado Plateau: implications for

602   biological soil crusts and soil processes. Plant and Soil 355:265-282.
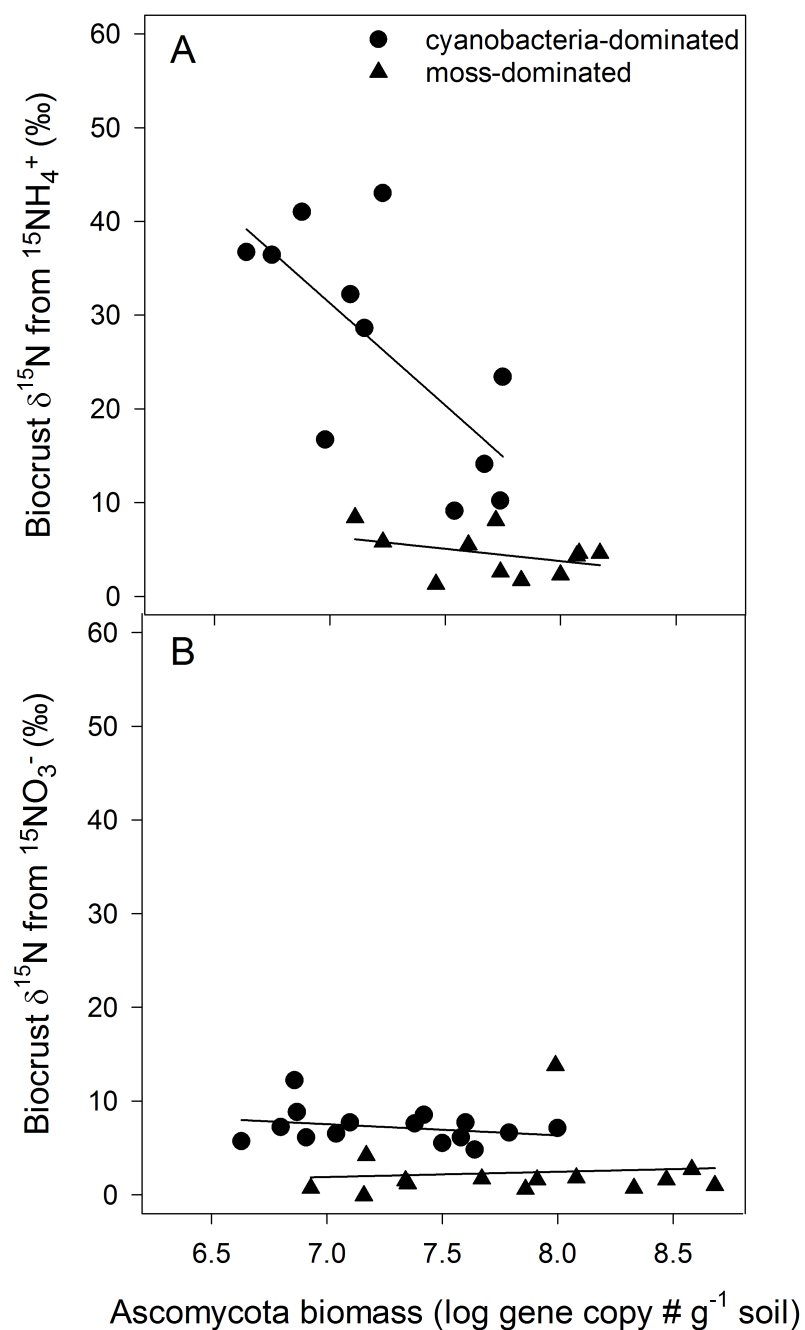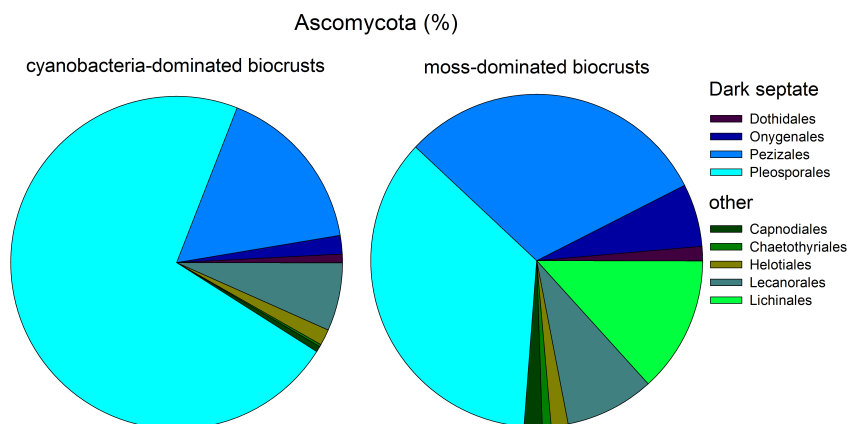

604

Figure 1

608   **Figure 2**

Figure 3

Ascomycota (%)

612